*Fracture 1977, Volume 3, ICF4, Waterloo, Canada, June 19 - 24, 1977*

# A FINITE ELEMENT ANALYSIS FOR DETERMINING DUGDALE MODEL SOLUTIONS OF CRACKED BODIES

K. J. Lau* and C. L. Chow**

## INTRODUCTION

In recent papers [1,2,3], the authors have introduced a conic-section simulation method of finding the stress intensity factor; the displacements on the crack surface calculated by the finite element analysis are used to match each segment on the crack surface with a segment on an equivalent ellipse corresponding to an opening crack in an infinite sheet under uniform tension [4]. That segment on the crack surface is then taken to provide an estimate for the stress intensity factor as quantified by the infinite sheet configuration. Mathematically, this may be expressed as

$$K = p' \sqrt{a_e'} \tag{1}$$

where $p'$ = uniform pressure in infinite sheet containing the simulating crack
$a_e'$ = half-crack length of the simulating crack

The matching can be effected either (i) by direct fitting of the displacements onto an elliptic curve with the crack tip as an apex [1,2], or (ii) by first fitting these displacements onto another conic-section (parabola or hyperbola) and then determining an equivalent ellipse which provides the same value for K through a relation between crack surface displacements and the strain energy release rate as described by Key [3,5]. The method has been proved to be of acceptable accuracy even when a relatively coarse finite element mesh and the simple constant-strain triangular elements are used in the finite element analysis.

Also based on the same infinite sheet crack configuration is the Dugdale strip yield model [6] characterized by the crack opening displacement [7]. In this model (Figure 1) an ideal elastic-plastic material is considered and the crack is assumed to deform elastically under the action of externally applied uniform tension $p_o$ with a tensile stress $\sigma_y$ acting over a hypothetical extension of length s at each end of the crack. $\sigma_y$ can be identified with the yield stress of the material. By superposition of the two stress fields and consideration of the finiteness of the stresses at the location of the hypothetical crack tip, it can be shown that the load/yield-stress ratio is given by [6]

$$\frac{p_o}{\sigma_y} = \frac{4}{\pi} \sin^{-1} \left(\frac{s}{2\, a_e}\right)^{1/2} = \frac{2}{\pi} \cos^{-1} \frac{a}{a_e} \tag{2}$$

*Hong Kong Polytechnic, Hung Hom, Hong Kong.
**University of Hong Kong, Pokfulam Road, Hong Kong.



MS22

and the COD is given by

$$\delta = \frac{8}{\pi}\,\varepsilon_y\, a \log \frac{a_e}{a} = \frac{8}{\pi}\,\frac{\sigma_y}{E}\, a \log\left(\sec \frac{\pi p_o}{2\sigma_y}\right) \tag{3}$$

where $\varepsilon_y$ is the elastic yield strain. By the relation between $\varepsilon_y$ and the overall strain on a given gauge length, critical COD-values can be applied to real structures for which the overall strains are easily measurable.

The present paper deals with the determination of the COD in cracks of arbitrary shape using the ellipse parameters in the K-determination through the conic-section approach. The advantage of the method is that both models have been built on the same Griffith crack geometry so that correspondence between p' and $p_o$, $a_e$' with $a_e$ in equations (1) and (2) makes the determination of COD just a convenient extension of the K-finding process.

## NUMERICAL DETERMINATION OF DUGDALE MODEL SOLUTION

In the original Dugdale model a crack in an infinite sheet was considered and the load/yield-stress ratio was obtained through the finiteness of the stresses at the hypothetical crack-tip region, which is equivalent to a cancellation effect between the elastic stress intensity factors due to the two stress fields $p_o$ and $\sigma_y$. In a cracked body of arbitrary shape, the same principle can be applied. Thus if the stress intensity factor $K_{Ip}$ due to the uniform pressure $p_o$ is expressed as

$$K_{Ip} = p_o\, a_e^{1/2}\, k_{Ip} \tag{4}$$

and the stress intensity factor $K_{Iy}$ due to a crack opening $\sigma_y$ at the crack tip region is expressed as

$$K_{Iy} = \sigma_y\, a_e^{1/2}\, k_{Iy} \tag{5}$$

where $k_{Ip}$ and $k_{Iy}$ are geometrical correction factors such that

$$k_{Ip} = k_{Ip}\left(a_e\right)$$

and $$k_{Iy} = k_{Iy}\left(a,\ a_e\right),$$

then according to the Dugdale's theory

$$K_{Ip} - K_{Iy} = 0,$$

or, from (4) and (5),

$$\frac{p_o}{\sigma_y} = \frac{k_{Iy}}{k_{Ip}} \tag{6}$$





The crack opening displacement can be found by superposition of the displacements obtained from the two finite element analyses, involving $p_o$ and $\sigma_y$ as

$$\delta_d{}^* = \delta_p{}^* \frac{k_{Iy}}{k_{Ip}} - \delta_y{}^* \tag{7}$$

where $\delta_p$* and $\delta_y$* are the crack surface separations due to unit magnitude of $p_o$ and $\sigma_y$ respectively, while $\delta_d$*, the superposed value, is the overall COD corresponding to unit magnitude of $\sigma_y$.

The above method of analysis was carried out by Hayes and Williams [8] using Bueckner's formulation [9] in the treatment of finite element analysis results, which is essentially an energy approach requiring at least two sets of finite element calculations for each loading system so that the Dugdale model solution for one particular combination of a and $a_e$ values necessitates four sets of finite element calculations. On the other hand, using the conic-section simulation approach, only two finite element analyses are necessary for any particular combination of geometry and loading system. Furthermore since both the Dugdale model and the conic-section analysis methods are built on the Griffith crack geometry, it is possible that closed-form solutions can be applied to reduce the amount of the finite element calculations. Specifically if the solution for the externally applied load for a particular value of $a_e$ is obtained, then the values of COD for different values of s can be calculated through the modifications of equations (2) and (3) so that no finite element calculation involving the $\sigma_y$ geometry is necessary. This is described in the following section.

## DUGDALE MODEL SOLUTIONS FROM SIMULATION ELLIPSE PARAMETERS

Three ways of implementing the ellipse parameters approach for the finding of COD are considered:

Method A: In the conic-section analysis applied to the displacements of two nearby points on the crack surface, the segment between these two points is matched with a segment on the Griffith crack opened by uniform pressure and having the same stress intensity factor K (Figure 2). The actual value of the surface displacement at the middle of the segment is preserved in the resulting simulation ellipse. Within this ellipse model, the superposition of a uniform tensile stress over a length s on the crack surface adjacent to the crack tip to produce zero value of resultant K can be quantified according to (2) as

$$\frac{s}{a_e{}'} = 2 \sin^2 \frac{\pi p_o{}'}{4\sigma_y{}'} \tag{8}$$

while the corresponding COD produced is given by (3) as

$$\delta = \frac{8}{\pi}\,\frac{\sigma_y{}'}{E}\, a' \log \frac{a_e{}'}{a'} \tag{9}$$

where various terms in the above equations are defined in Figure 2. Returning to the actual crack under consideration, the necessary value of the stress $\sigma_y$ in the region s to produce the stress intensity factor will be different from $\sigma_y$', but the value of the COD should remain the same, subject to the validity of two assumptions; firstly, the displacements of the points $P_1$ and $P_2$ (Figure 2) must be truly representative of the crack tip stress intensity factor; secondly, the crack shape produced by uniform stress $\sigma_y$ in region s in the real crack system should be functionally similar to that produced by a uniform stress $\sigma_y'$ in the region s of the model system.

Method B: Each simulation ellipse corresponding to a segment on the actual crack surface is considered in turn with respect to a given value of s. The effective change in crack surface separation at r = s produced by $\sigma_y'$ over the length s is calculated as

$$\delta_y = \frac{4p_o'a_e'}{E}\left(1 - \frac{a'^2}{a_e'^2}\right)^{1/2} - \frac{8}{\pi}\frac{\sigma_y'}{E} a' \log \frac{a_e'}{a'} \qquad (10)$$

where the first term on the right hand side is the separation due to $p_o'$ alone and the second term is the COD as given by equation (3). An average is taken of the $\delta_y$-values from all the simulating ellipses and the crack opening displacement is then evaluated as the difference between the crack surface separation produced by the actual load applied as calculated by the finite element analysis, (interpolated if necessary) and the average $\delta_y$-value. This method is in principle the same as method A except that the effective stress intensity factor is now taken as the average value represented by the whole crack profile. Furthermore this method is more convenient for treating values of s that do not match with the nodal positions of the finite element mesh used. There is however one minor restriction in that the $a_e'$-values of the simulation ellipses at points close to the hypothetical crack tip may sometimes fall short of s so that in some extreme cases, sufficient $\delta_y$-values may not be available to give a good average value.

Method C: Both methods A and B are subject to the assumption that equation (10) governs the change in crack surface separation due to $\sigma_y$ on the actual crack surface. To check whether this equation based on the original Dugdale model adequately represents the crack profile produced, a more practical assumption is considered - that the ratio of the displacements due to the two sets of loadings in the actual system remains the same as that in the model system. Since the displacements are to be produced by the loading systems giving the stress intensity factors of equal magnitude as reflected in an opening displacement, the effects of finite width, etc., on these representative displacements should be equal. Hence in this third method, a ratio of displacements is obtained as

$$\frac{\delta_y}{\delta_p} = 1 - \frac{\dfrac{8\sigma_y'}{\pi E} a' \ell n \dfrac{a_e'}{a'}}{\dfrac{4p_o'a_e'}{E}\left(1 - \dfrac{a'^2}{a_e'^2}\right)^{1/2}} \qquad (11)$$

whence the COD can be found as the product of $(1 - \delta_y/\delta_p)$ and the actual displacement $\delta_p$ obtained by the finite element analysis.

In the above methods the COD-values are found with no reference made to the load/yield-stress ratio in the actual system. An approximation process is now used to transfer the value of $\sigma_y'$ in the model system to that





of $\sigma_y$ in the actual system by using the correction factors of some standard configurations. Thus $\sigma_y$ is estimated as

$$\frac{\sigma_y'}{\sigma_y} = k_1 (s, W - a) \qquad (12)$$

where $k_1$ corresponds to the mode I correction factor function $k_I(a_e, W)$ of the fully loaded crack in a plate of finite width 2W.

## DISCUSSIONS AND CONCLUSIONS

Due to the space restriction in this presentation, only the results obtained for a centrally cracked finite-width plate geometry are presented. Results for other configurations can be found in [10] and the COD-values by the methods A and B are compared in Figure 3 in dimensionless form as

$$\delta^* = \frac{E}{p_o W}\,\delta \qquad (13)$$

It can be seen that remarkable agreement in the computed results has been achieved except for the combinations of the high $a_e/W$ and $s/a_e$ values. The reason for the disparities is probably that finite-width effect in these cases renders the displacements of the points remote from the crack tip inadequate in the representation of the crack-tip stress intensity factors. Method B is expected to produce more reliable results in these cases provided that sufficient $\delta_y$-values are made available for the averaging process. This provision is found to have been largely satisfied except for only a few extreme cases. The results from method C are found to be practically co-incident with those from method B for most cases so that, for clarity of the plotting, they are not shown in the same graph, but are given in Table 1 together with those of method B and the results from reference [8]. Also shown in the table are the estimated values of the load/yield-stress ratio. Since satisfactory agreement can be observed between the results of the present method and that of Hayes and Williams [8], it may be inferred that conceptually similar processes have been executed in relating the stress ratio to the plastic zone size through equating the magnitudes of the K-values from the two stress systems. Comparison of the COD values reveals that appreciable disagreement between the methods B and C exists only at the high $s/a_e$ values and a/s = 0.1 or 0.2, i.e. when the plastic zone length is much larger than that of the actual crack length. This establishes the validity of equation (10) as mentioned earlier. Comparison with the COD-values given by Hayes and Williams show rather disappointing discrepancies. One major problem in both approaches is that the COD is seldom a large fraction of the displacement due to the external applied stress system so that small percentage error in the displacement calculations may become magnified in the COD-values. From the nature of the finite element mesh used by Hayes and Williams, which consists of coarse grids with constant element width along the line of the crack length, underestimates of the displacements are expected. This probably explains the discrepancies between the COD-values for the central crack case. Nevertheless agreement in the results may be considered as satisfactory when the plastic zone size is not too large as compared with the actual crack size while the accuracy of each method depends heavily on the accuracy of the displacements obtained. The present methods via the conic-section analysis follow closely the original idea of representing a crack-tip strain field by an opening displacement. Agreement among the three methods of implementation lends credibility to the principle used and the practically constant values of $\sigma_y'$ and $\delta_y$ from different simulation ellipses for different sections of the crack surface in practically all cases under consideration, as exemplified by Table 2, further confirm the validity of the method.

## REFERENCES


1. CHOW, C. L. and LAU, K. J., J. Strain Analysis 11, 1976, 1.
2. CHOW, C. L. and LAU, K. J., Int. J. Fracture 12, 1976, 1.
3. CHOW, C. L. and LAU, K. J., Int. J. Fracture 12, 1976, 5.
4. SNEDDON, I. N. and ELLIOT, H. A., Quart. Appl. Math. 4, 1946.
5. KEY, P. L., Int. J. Frac. Mech. 5, 1969.
6. DUGDALE, D. S., J. Mech. Phys. Sol. 8, 1960.
7. WELLS, A. A., Proc. Cranfield Crack Propagation Symposium, Vol. 1, 1961.
8. HAYES, D. J. and WILLIAMS, J. G., Int. J. Frac. Mech. 8, 1972.
9. BUECKNER, H. F., Trans. A.S.M.E. 80, 1958.
10. LAU, K. J., Ph.D. Thesis, University of Hong Kong, 1975.






Table 1 COD for Centrally Cracked Plate in Uniform Tension, H/W = 3.5

| a/W | s/a | $\delta^*$ | | | $P_o/\sigma_y$ | |
|---|---|---|---|---|---|---|
| | | Method B | Method C | Hayes & Williams 1972 | Present Method | Hayes & Williams 1972 |
| 0.1 | 0.5000 | 0.2666 | 0.2317 | 0.2471 | 0.6344 | 0.6406 |
| | 0.6667 | 0.3712 | 0.3996 | 0.3449 | 0.7457 | 0.7662 |
| | 0.7500 | 0.4455 | 0.5390 | 0.4109 | 0.8140 | 0.8208 |
| | 0.8000 | 0.5669 | 0.6321 | 0.4623 | 0.8304 | 0.8559 |
| | 0.8333 | 0.6116 | 0.7702 | 0.5054 | 0.8523 | 0.8690 |
| | 0.8572 | 0.6977 | 0.9017 | 0.5421 | 0.8686 | 0.8808 |
| | 0.8750 | 0.5853 | 0.7795 | 0.5768 | 0.8898 | 0.8887 |
| | 0.8889 | 0.9805 | 1.2950 | 0.6120 | 0.9388 | 0.8944 |
| 0.2 | 0.3333 | 0.3876 | 0.3825 | 0.3680 | 0.4879 | 0.4996 |
| | 0.5000 | 0.5760 | 0.5997 | 0.5247 | 0.6124 | 0.6322 |
| | 0.6400 | 0.7290 | 0.7639 | 0.6366 | 0.6728 | 0.6981 |
| | 0.6667 | 0.8750 | 0.9637 | 0.7269 | 0.7112 | 0.7367 |
| | 0.7143 | 1.0620 | 1.1840 | 0.8051 | 0.7408 | 0.7610 |
| | 0.7500 | 1.1676 | 1.3316 | 0.8775 | 0.7699 | 0.7772 |
| | 0.7778 | 1.0604 | 1.1653 | 0.9540 | 0.8290 | 0.7889 |
| 0.3 | 0.2500 | 0.5016 | 0.5091 | 0.4725 | 0.4024 | 0.4125 |
| | 0.4000 | 0.7621 | 0.7686 | 0.6821 | 0.5295 | 0.5359 |
| | 0.5000 | 0.9837 | 1.0238 | 0.8364 | 0.5751 | 0.6008 |
| | 0.5714 | 1.2638 | 1.3169 | 0.9663 | 0.6074 | 0.6400 |
| | 0.6250 | 1.5420 | 1.6323 | 1.0845 | 0.6450 | 0.6654 |
| | 0.6667 | 1.6700 | 1.6936 | 1.2093 | 0.7128 | 0.6835 |
| 0.4 | 0.2000 | 0.6090 | 0.6163 | 0.5786 | 0.3376 | 0.3477 |
| | 0.3333 | 0.9670 | 0.9738 | 0.8432 | 0.4384 | 0.4574 |
| | 0.4386 | 1.3100 | 1.3368 | 1.0452 | 0.4923 | 0.5166 |
| | 0.5000 | 1.6840 | 1.7558 | 1.2237 | 0.5305 | 0.5529 |
| | 0.5556 | 2.1171 | 2.1211 | 1.4079 | 0.5924 | 0.5776 |
| 0.4 | 0.1667 | 0.7471 | 0.7550 | 0.6980 | 0.2852 | 0.2935 |
| | 0.2857 | 1.2239 | 1.2307 | 1.0290 | 0.3690 | 0.3879 |
| | 0.3750 | 1.7363 | 1.7646 | 1.2941 | 0.4164 | 0.4392 |
| | 0.4444 | 2.4278 | 2.4276 | 1.5564 | 0.4632 | 0.4717 |
| 0.6 | 0.1428 | 0.9281 | 0.9314 | 0.8492 | 0.2383 | 0.2444 |
| | 0.2500 | 1.6165 | 1.6163 | 1.2717 | 0.3066 | 0.3226 |
| | 0.3333 | 2.5103 | 2.4953 | 1.6484 | 0.3606 | 0.3655 |
| 0.7 | 0.1250 | 1.2234 | 1.2279 | 1.0644 | 0.1917 | 0.1970 |
| | 0.2222 | 2.3148 | 2.2529 | 1.6485 | 0.2519 | 0.2585 |
| 0.8 | 0.1111 | 1.8185 | 1.8127 | 1.4364 | 0.1466 | 0.1483 |

Table 2 $\sigma_y'$ and $\delta_y^*$ Values Obtained from Method B

| $r/a_e$ | $a_e'/a_e$ | $\sigma_y'/p_o$ | $\delta_y^*$ |
|---|---|---|---|
| 0.1667 | 2.4593 | 1.6960 | 1.581 |
| 0.2250 | 1.3611 | 1.6933 | 1.656 |
| 0.3000 | 1.1268 | 1.6967 | 1.704 |
| 0.3917 | 1.0401 | 1.7018 | 1.734 |
| 0.4958 | 1.0066 | 1.7061 | 1.751 |
| 0.6083 | 0.9841 | 1.7111 | 1.764 |
| 0.7500 | 0.9720 | 1.7152 | 1.773 |
| 0.9167 | 0.9761 | 1.7130 | 1.769 |

$s/a = 1.4$, $a_e/W = 0.6$, $\delta_p^* = 2.700$

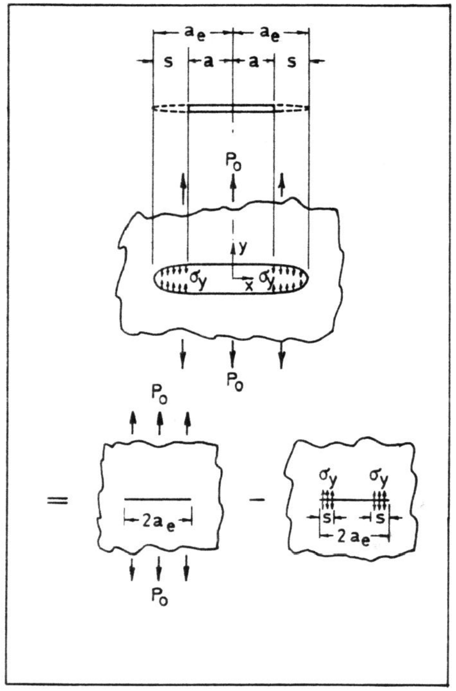


Figure 1 Geometry of Slit and Equivalent System for Dugdale Model





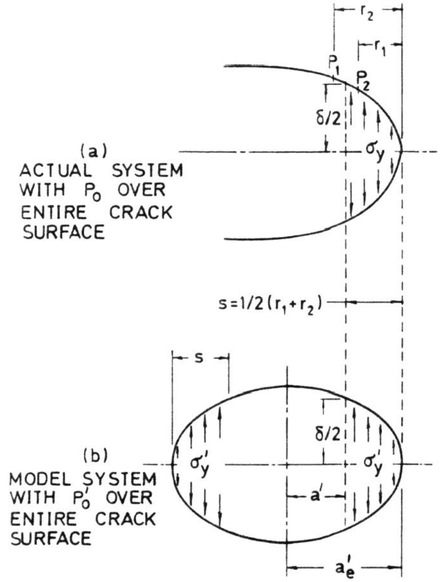


Figure 2 Actual Crack Shape and Simulation Model System

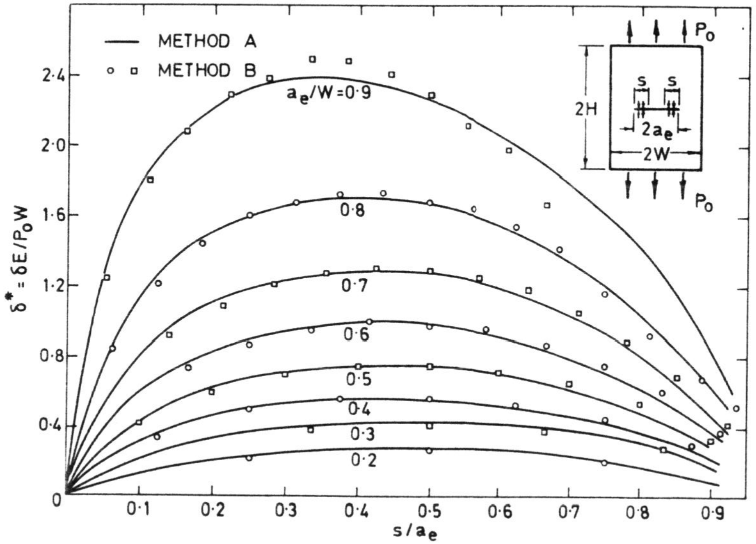


Figure 3 COD for Central Crack Under Uniform Tension, $H/W = 3.5$